

## **High-resolution Monitoring at Parkfield**

Grant Number: 01HQGR0057

**T.V. McEvilly**, University of California, Berkeley Seismological  
Laboratory 475 McCone Hall, Berkeley, CA 94720-4767

Telephone: (510) 642-4494; Fax: (510)643-5811; E-mail: tom@seismo.berkeley.edu

**NEHRP Elements: II, III**

**Key Words:** seismology, Tectonophysics, Seismotectonics, Earthquake forecasting

### **INVESTIGATIONS UNDERTAKEN:**

This research began with NEHRP in 1986 as a proposed direct test with proven and modern technology of two hypotheses critical to our understanding of the physics of the earthquake process and the possibilities for short-term earthquake prediction:

- 1) That the earthquake nucleation process produces stress-driven perturbations in physical properties of the rocks in the incipient focal region that are measurable, and
- 2) That the nucleation process involves progressive and systematic failure that should be observable in the low-magnitude microseismicity with high-resolution locations and wave propagation attributes.

The data acquired in this experiment are unique and they are producing results that force a new look at some conventional concepts and models for earthquake occurrence and fault-zone dynamics. Analyses of the resulting nine years of Parkfield monitoring data have revealed significant and unambiguous departures from stationarity both in the seismicity characteristics and in wave propagation details for paths within the presumed M6 nucleation zone where we also have found a high Vp/Vs anomaly at depth, a region of high FZGW generation, and where the three recent M4.7-5.0 sequences have occurred. Synchronous changes well above noise levels have also been seen among several independent parameters, including seismicity rate, average focal depth, characteristic sequence recurrence intervals, fault creep and water levels in monitoring wells. The significance of these findings lies in their apparent coupling and inter-relationships, from which models for fault-zone structure and process can be developed and tested with time. The more general significance of the project is its production of a truly unique continuous baseline, at very high resolution, of both the microearthquake pathology and the subtle changes in wave propagation.

### **RESULTS:**

In a series of thirteen journal articles since 1991 we have presented the evolution of a new and exciting picture of the San Andreas fault zone system responding to its plate-boundary loading. Our efforts over the past year have focused on the upgrade and expansion of the High Resolution Seismic Network (HRSN) to collect very low magnitude events at a completeness threshold of -1 in the region surrounding the SAFOD target and on advanced research in the areas of earthquake physics, event relocations and detailed seismic structure, magnitude and source parameter scaling, Fault Zone Guided Wave (FZGW) generation and propagation, and spatial and temporal variations in seismic anisotropy and fault slip rates at depth along the SAF including and north of the Parkfield region.

#### **Network Upgrade and Expansion**

Thanks to emergency funding from the USGS NEHRP, we have replaced the original 10-station system with a modern 24-bit acquisition system (Quanterra 730 digitizers, advanced software using flash disk technology, spread-spectrum telemetry, Sun Ultra 10/440 central processor at the in-field collection point, with 56K frame-relay connectivity to Berkeley). The new system is now online and recording data continuously at a central site located on the California Department of Forestry (CDF) fire station in Parkfield. A microwave link was installed to support the current IRIS PASSCAL broadband array deployment in Parkfield, and is shared by the HRSN and PASSCAL. All HRSN data are recorded to disk at the CDF site. A modified version of the REDI real-time system detects events from the HRSN data, creates event files with waveforms from the HRSN and PASSCAL networks, and sends the event data in near real-time to UC Berkeley. The upgraded system is compatible with the data flow and archiving common to all the elements of the BDSN/NHFN and the NCEDC, and is providing remote access and control of the system. It is also providing data with better timing accuracy and longer records which are to eventually flow seamlessly into NCEDC. The new system solves the problems of timing resolution, dynamic range, and missed detections, in addition to providing the added advantage of conventional data flow (the old system

recorded SEG-Y format). Significant efforts were made to identify and reduce noise sources arising from the new recording, telemetry and site design. The most significant contributors to noise have been identified and fixes have been developed and implemented at the 6 critical stations surrounding the SAFOD drilling target. Fixes for the remaining 7 stations, (some requiring the purchase of additional equipment) is currently underway. Identification and development of fixes for the lesser noise sources is continuing.

At this time data streams on all components are being recorded continuously at 20 and 250 sps. These data are being archived on DLT tape, and 6, 250 sps vertical channels from the critical stations surrounding the SAFOD drilling target are being continuously sent to Berkeley over the frame relay-circuit for purposes of fine tuning the triggering algorithm for detection at the smallest possible magnitude levels. Plans are to replace the continuous archiving of 250 sps data with the triggered data event gathers which are to be sent in near real time to Berkeley over frame relay to be archived on the NCEDC. Plans are to replace the 6, 250 sps data with continuous 20 Hz data for investigations of borehole based very high frequency teleseismic and regional event investigations and to archive these data on the NCEDC as well. A first cut version of the new triggering scheme being developed has been implemented and is already detecting earthquakes at an increased rate--about 3 times the number of earthquakes detected before the upgrade.

We have also added three new borehole stations at the NW end of the network as part of the deep fault-zone drilling (San Andreas Fault Observatory at Depth - SAFOD) project, with NSF support, to improve resolution at the planned drilling target on the fault. **Figure 1** illustrates the location of the proposed drill site, the original 10 HRSN stations, the three new borehole stations and relocated seismicity. The three new stations use similar hardware to the main network, with the addition of an extra channel for electrical signals. We are also using the HRSN triggering algorithm in a joint triggering scheme with the PASSCAL network to allow that 60-station surface array to identify events on the lower noise, greater sensitivity of the borehole network. This will significantly increase event detection and reduce false triggers for the 60-station network data.

Shown in **figure 2** are waveforms (before filtering) from a magnitude 0.0 earthquake and 2 of its after shocks (magnitudes -0.8 and -1.3) as recorded on stations of the short period regional NCSN and local 3-component borehole HRSN. All three of these earthquakes occurred within a 31 minute time period on Sept. 1, 2001. The 2 aftershocks have estimated magnitudes -0.8, and -1.3 respectively, They are not part of the NCSN catalog. The greater detection threshold of the borehole HRSN has many important implications for studies of earthquake and fault physics, for imaging, monitoring, scaling, earthquake hazards and for fault slip rates at depth. The NCSN archive generally does not contain horizontal short period velocity seismograms for events in this area. Unlike the NCSN short period array, all HRSN stations record 3-component velocity data. The HRSN horizontal components give much better definition of the S-arrival than the vertical components alone. The apparent S-phase as seen on the vertical components (designated "A") arrives significantly later than the S-phase arrival seen on the horizontal components ("A"). The arrow on the uppermost record shows the NCSN S arrival time pick which was used by the USGS for locating the M0.0 event. This pick is approx. 0.25 to 0.5 seconds later than what would be picked using the horizontal components of the HRSN. Arrival time errors of this magnitude can lead to location errors on the order of 2 to 3 km. Depth of the M0.0, as given in the NCSN catalog, is 12.28 km. The apparent S in the vertical records might be attributable to near surface back scattered energy or possibly to Fault Zone Guided Wave arrivals--known to exist at Parkfield.

All 39 channels of the upgraded and expanded 13 station HRSN are currently recording data. An example of 3-component seismograms of the M-0.8 and M-1.3 aftershocks recorded at one of the 3 recently added stations (CCRB) are shown at the bottom of figure 2. Multiple arrivals at numerous well distributed stations insure that events can be accurately located even at very low magnitudes and at relatively great depth. Extrapolation using assumed geometrical spreading and the added benefit gained by filtering of the waveforms suggests that events with magnitudes below M-2.0 will be detected and located in proximity of the SAFOD target.

### **Relocations and Detailed Structure**

We explored the degree of improvement possible over the Michelini and McEvelly (1991) 3-D P- and S-wave velocity models estimated early in the Parkfield project, where there were only 169 events used in the inversion. Now, with another decade of data, it is possible to build a much more extensive data set. About 4800 and 2100 P and S arrival times, respectively, were selected for uniform raypath illumination throughout the study volume. The gross features of the new model are similar to the 1991 model; however, the new model includes a larger geographic scope and additional auxiliary data sets. The additional data primarily help to fix the edges of the

model and to extend the model in the along fault direction (both NW and SE). As a result, the event locations on the ends of the network have straightened out significantly (including the those in the vicinity of the SAFOD drilling site). The apparent dip of the events is reduced somewhat, but the hypocenters are still biased to the SW of the fault trace and the USGS locations.

To further improve resolution of the hypocenter distribution at Parkfield, we are collaborating with Alberto Michellini at the Istituto Nazionale de Oceanografia e di Geofisica Sperimentale in Italy to extend the double-difference (DD) relative relocation method (Waldhauser et al., 1999) to the 3-D case. In a focused study of the target zone of the SAFOD deep drilling project, we found the comparable measures of resolution for the three commonly used high-resolution location methods - catalog solutions from the NCSN using a 1-D velocity model, catalog solutions from the HRSN using a 3-D velocity model, and DD relative locations based on HRSN arrival times, and HRSN waveform-correlation data - based on the scatter of events in repeating sequences, to be 1000 m, 180 m and 6 m, respectively (**figure 3**). It appears the SAFOD exercises aimed at hypocenters will need to rely upon the cross-correlation method for accurate relative locations, and that the constellation of events within the drilling target will have to be precisely fixed using direct travel time measurements made to or from the pilot and main boreholes at various depths.

Another notable finding of the focused study has been the discovery of two subparallel, seismically active fault strands of the SAF separated by about 300 m and oriented--perpendicular to the horizontal drilling direction planned by SAFOD. The M2 repeating earthquake sites targeted by SAFOD occur on the NE strand--furthermost away from the drill rig--so that the horizontal component of drilling will have to penetrate the active SW strand first and remain intact during drilling into the NE strand and during subsequent monitoring and coring phases of the experiment.

#### **Earthquake Physics and Spliced Magnitude Catalog:**

Scaling laws for earthquake source properties, statistical description of earthquake occurrence, precise monitoring, forecasting, estimation of fault slip rates from repeating microearthquakes, or virtually any careful analysis of the earthquake process all demand an accurate estimation of earthquake size. The difficulty is that these kinds of investigations must operate at the  $M \sim 0$  level to acquire sufficient data over the lifetime of a realistic study. For example, at  $M \sim 6$  on the Parkfield San Andreas segment, definition of the recurrence statistics for repeating rupture requires data spanning centuries, while at  $M \sim 0$ , the same number of events can be seen in 2-3 years, and furthermore there are hundreds of such repeating sequences occurring along a similar length segment of the fault. For the Parkfield data we have compiled and carefully tested methodologies for estimating seismic moment and for calibrating the HRSN moments with the regional NCSN preferred magnitude catalog using order statistics. The result has been a seamless relationship and catalog of earthquake magnitudes from  $M < 0$  to  $M 6$ .

Data from this catalog are being used in current collaborative efforts with researchers at USC (C.G. Sammis) and the Univ. of Alaska (M. Wyss) that require accurately merged catalogs to explore the relationship between fractal dimension,  $D$ , and  $b$ -values on locked and creeping sections of the San Andreas Fault (Sammis et al., in prep.). The data are also being used to refine the empirical scaling relationship between magnitude, repeat times and slip loading rates (Nadeau and Johnson, 1998 and Nadeau and McEvilly, 1999) and to calibrate and integrate estimates of slip rate at depth from repeating earthquakes at Parkfield with surface deformation and repeating earthquake data elsewhere on the central San Andreas, Calaveras and Hayward faults (Nadeau and McEvilly, 2000; Burgmann et al., 2000). Both the  $D$  and  $b$ -values and the scaling factor relating the two ( $d/c$ ) differ significantly between the locked and creeping sections of the fault. Theoretical considerations that assume constant stress drop scaling predict  $d/c$  to be 2--a value which fits the estimates in the asperity region only. Using the stress drop scaling proposed by Nadeau and Johnson (1998),  $d/c = 1.5$ --inclusive of both the asperity and creeping fault data, though just barely.

Since last year several studies have been published that attempt to explain the striking scaling relation of repeat times from characteristic microearthquake sequences with sequence event size. The original scaling for Parkfield microearthquakes was first published in a peer reviewed journal by Nadeau and McEvilly (1997), and later developed in more detail and extended to include larger repeating earthquakes by Nadeau and Johnson (1998). These analyses presented strong evidence in support of a highly heterogeneous fault zone with scale-dependent stress drops. The recent publications take issue with the interpretations of heterogeneity of the fault zone and propose various alternative fault-zone processes--such as load-shielding (Anooshehpour and Brune, 2000; Sammis and Rice, 2000), creep-slip (Beeler, 2000) or rupture overlap (Schaff et al., 2001) to avoid the high stress drops we hypothesized for the small events.

Coincidentally, ongoing work at Berkeley correlating the energetics of formation of fossil earthquakes (i.e.

pseudotachylites) with repeating earthquakes at Parkfield has evolved to the point where strong arguments can be made based on direct field observation of features of exhumed fault zones to support the stress drop scaling and strong and scale-dependent, heterogeneity of fault strength. (Wen et al., 2000; Nadeau et al., 2001).

An static asperity model of earthquakes has also been developed that explains the scale-dependent relationships for the repeating earthquakes (Johnson and Nadeau, 2001). The model leads to differential equations that can be solved to yield a complete static model of an earthquake--equations for scalar seismic moment, the dimension of the strong asperity patches and of the earthquake rupture and displacement shadow surrounding the asperities are all specified as functions of a displacement deficit that accumulates between repeated rupture. The model predicts a repeat time scaling for the earthquakes that is in agreement with the empirical results for repeating earthquakes and, assuming that the asperity patches are distributed on the fault surface in a random fractal manner, leads to a frequency-size distribution of earthquakes that agrees with the Gutenberg-Richter formula and a simple relationship between the b value and fractal dimension, D. The model has also shown that the basic features of the static model can be used to simulate dynamic rupture with numerical calculations employing the boundary integral method. These simulation procedures are currently in development.

A study of source area with seismic moment that includes pore pressure effects is also being pursued in collaboration with Stephen Miller of the Swiss Federal Institute of Technology in Switzerland. Results are preliminary but appear to show a good scaling from the very small microearthquakes at Parkfield ( $M < 0$ ) through to very large earthquakes ( $M > 7$ ) and suggest that pore pressure may play the dominant role in determining fault strength and earthquake recurrence.

#### **Propagation: Fault-Zone Guided Waves and Temporal Changes using Microearthquakes:**

There has been a lot made of so-called fault-zone guided waves (FZGW). Much of it has been directed toward modeling wave propagation in relatively simple, vertical low-velocity structures in order to match discrete observations of the late, low frequency arrivals sometimes recorded near the fault trace. We are approaching this problem from a somewhat different direction, using the extensive observations of these waves in the Parkfield network, our 3-D P- and S-velocity models for the fault zone, Vibroseis results (Karageorgi et al., 1992, 1997; Korneev et al., 2000), and a tomographic inversion of the 3-component FZGW arrivals from microearthquakes. The tomographic inversion has greatly facilitated the characterization of the distribution of FZGW generation throughout the zone. It uses source-receiver paths from the thousands of microearthquakes at Parkfield recorded by the HRSN.

The goals of this research are to determine the patterns of generation and propagation of FZGW, to characterize the wavefield in terms of velocity attenuation and particle motion relative to the fault zone, and to model the phenomenon numerically using new 3-D guided-wave algorithms under development. We also take advantage of the numerous and widely distributed sites of repeating earthquakes as repeating illumination sources to monitor temporal changes in FZGW propagation to search for evidence relating to the processes of fault healing and large event nucleation.

Initial results suggest that strong generation and propagation of FZGWs are controlled by a well-defined feature within the fault zone that is high Q and appears to be the plunging along the NW edge of the M6 asperity at the transition boundary between locked and creeping fault slip at depth. The velocity, Q and FZGW generation characteristics suggest that this zone is a region of dewatering caused by fracture closure and/or fault-normal compression.

Deep characteristic microearthquake sources generally show little variation in their waveforms through time, suggesting that any propagation changes due to relatively deep (>3-4km) fault zone processes are small. Nonetheless, small systematic changes do appear to exist at the resolution limits of the current data set, especially for split shear wave arrivals. In collaborative work with Paul Silver and Fenglin Niu at Carnegie, we are exploring these fine scale systematics more thoroughly using advanced techniques to improve the resolution of the data. The goal is to characterize the apparent changes at the highest resolution possible and to investigate their relationship to the structure and observed deformation patterns of the fault at Parkfield. Early results are to be presented at the 2001 Fall meeting of the American Geophysical Union in San Francisco, CA.

#### **Fault Slip Rates at Depth from Characteristic Microearthquakes:**

We continue to monitor fault slip rates at depth using characteristic microearthquake sequences recorded on both the HRSN and NCSN at Parkfield and have recently extended the analysis to a regional Scale using available NCSN data recorded along an 170 km long stretch of the SAF that includes the Parkfield segment and extends northward to the southern terminus of rupture of the 1989 Loma Prieta (LP) earthquake. The microearthquakes provide the best spatial coverage along most of the creeping section of the SAF because the

density of creep meters there is low. Observed features of slip rates show systematics in slip rate variation that are quasi-periodic in the central creeping section. These variations appear to be absent near the LP terminus until after LP event, when the periodic pattern appears as a superposed slip signal riding on the exponential afterslip decay of LP. Migration pulses also appear to be feeding into the Parkfield area from the central creeping section at rates of about 25 km/yr. The migration pulses entering Parkfield do not appear to continue through the Parkfield area suggesting further accumulation of stress is taking place.

#### **NON-TECHNICAL SUMMARY:**

We have completed the upgrade and expansion of the borehole HRSN at Parkfield and are in the process of reducing noise sources associated with the new equipment and installations. We are also refining the event triggering scheme to detect events as small as -2M. We continue to operate and maintain the network as well and to collect and archive the data at the NCEDC facility in Berkeley. Various studies continue to search for precursory changes in material properties and slip deformation within the preparation zone of the expected next M6 Parkfield earthquake and to advance our understanding of the failure process on this section of the San Andreas fault. Detailed studies of the seismic structure and systematics of slip at depth in the vicinity of the SAFOD drilling target are also continuing as are investigations into a variety of subjects related to understanding EQ physics, Scaling and the FZGW phenomena.

#### **REPORTS PUBLISHED:**

- Nadeau, R.M. L.R. Johnson and H.-R. Wenk, Pseudotachylites as Fossil Earthquakes, *Seismol. Res. Letts.*, in revision, 2001.
- Johnson, L.R., and R.M. Nadeau, Asperity Model of an Earthquake - Static Problem, *Bull. Seismol. Soc. Am.*, in press, 2001.
- Korneev, V.A., T.V. McEvelly, and E.D. Karageorgi, Seismological studies at Parkfield VIII: Modeling the observed travel-time changes, *Bull. Seismol. Soc. Am.*, 90(3), 702-708, 2000.
- McEvelly, T.V., V.A. Korneev and R.M. Nadeau, Seismological Studies at Parkfield IX: Characteristics of Fault-zone Trapped Waves, in prep., 2001.

#### **DATA AVAILABILITY:**

The Parkfield waveform data and hypocenter catalog are accessible through the Northern California Earthquake Data Center (URL: <http://quake.geo.berkeley.edu/hrsn/hrsn.archive.html>). Absolute time is a problem in the early operation of the network and when there have been outages of the time code system, so that the data cannot be merged indiscriminately with NCSN data. Data archives have been maintained also by Peter Malin (Duke University) and for much of the experiment data were also recorded by the USGS on their Microvax-Metrum system. Contact: [tom@seismo.berkeley.edu](mailto:tom@seismo.berkeley.edu)

**Figure 1.** Map showing the San Andreas Fault trace, the location of the original 10 Parkfield HRSN stations (filled diamonds) and the 3 new sites (open diamonds), along with the BDSN station PKD (filled square). Seismicity is also shown (gray points) and the locations of the 8 source points for the Vibroseis wave propagation monitoring experiment are represented by small black triangles. The epicenter of the 1966 M6 Parkfield mainshock is located at the large open circle. The location of the proposed SAFOD drill site is shown by the filled star. Station GHI (Gold Hill, not shown) is located on the San Andreas Fault about 8 km to the Southeast of station EAD.

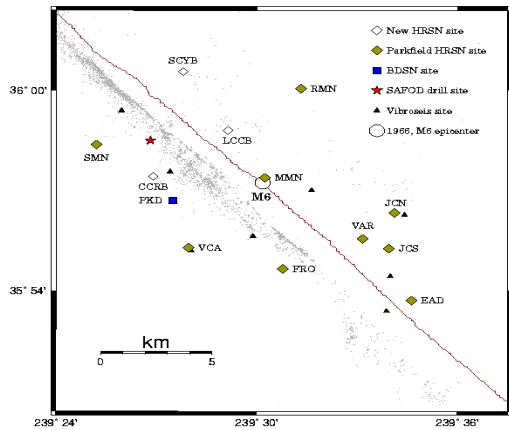


Figure 2 (left). Shown are unfiltered waveforms from a magnitude 0.0 earthquake and 2 of its after shocks (magnitudes -0.8 and -1.3). The P and S phase arrivals are indicated as P1, P2, P3 and S1, S2, S3 for magnitude 0.0, -0.8, and -1.3 events respectively. Uppermost seismogram is the M0.0 quake recorded by the NCSN vertical short period surface station PVC (component VHZ) located in Vineyard Canyon near Parkfield. Second seismogram is the same event recorded on vertical component channel (DP1) by the HRSN borehole station VCAB. The PVC-VHZ data are sampled at 100 sps and VCAB-DP channels at 250 sps. PVC is 78 meters from VCAB. Third seismogram contains waveforms of the M-0.8 and M-1.3 aftershocks recorded on VCAB-DP1 (phases P2 and P3). These events occurred 6.7 seconds apart. Aftershock records are scaled x5 to aid in the comparison. Horizontal seismograms from VCAB (components DP2 and DP3) are shown in the subsequent four seismograms for all 3 events.

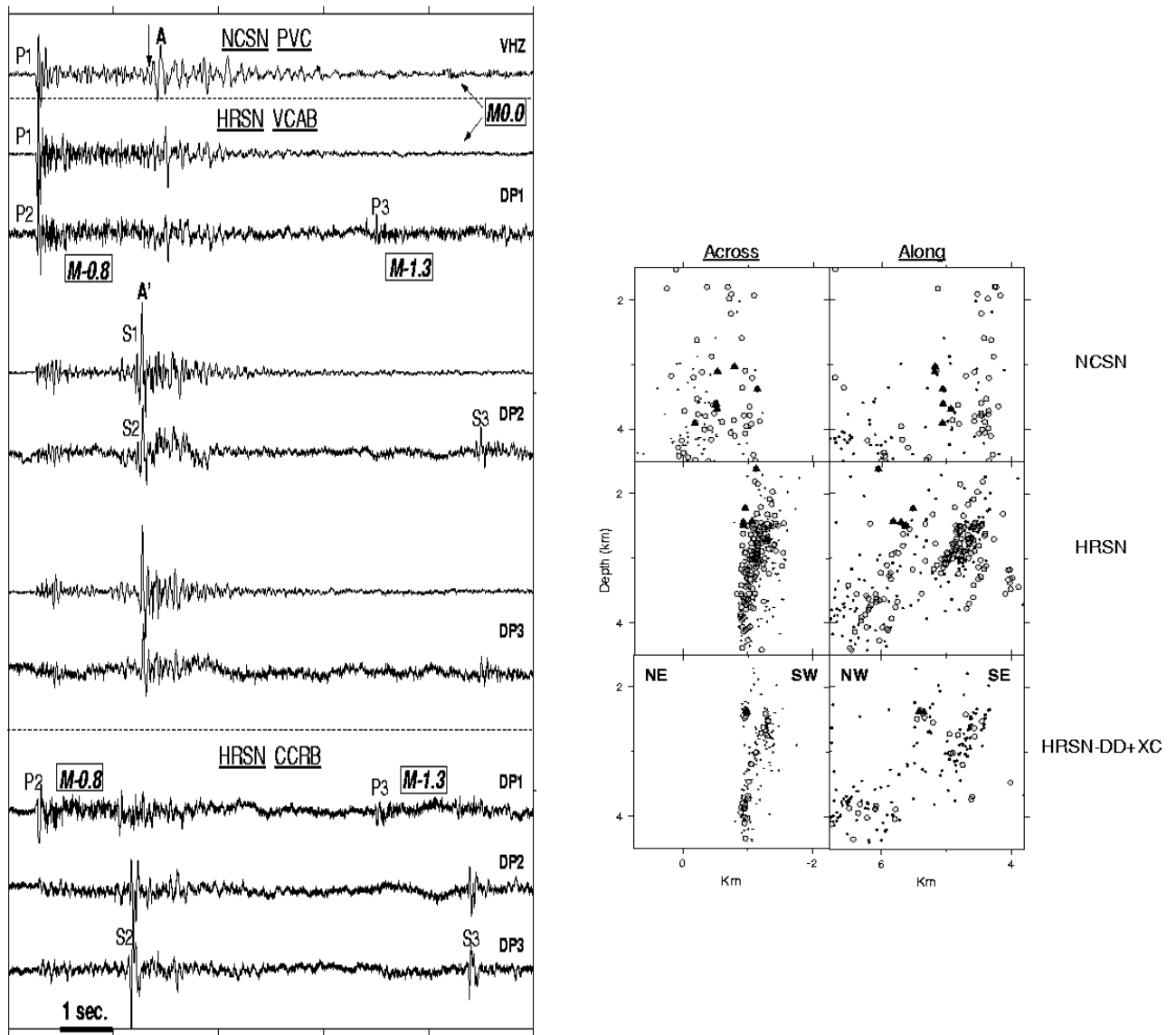


Figure 3 (right). Enlargement of a 3x3 km region about the proposed SAFOD drilling target. Light gray circles show locations of 144 individual characteristically repeating micro-earthquakes from 31 sequences. Black triangles show locations of events from the 2 additional repeating M2 sequences proposed as SAF penetration targets by SAFOD. At lower resolution the repeating quake locations scatter widely. As resolution increases, their locations collapse onto the 33 sites of repeating activity shown in the bottom panels. Black dots are locations of non-repeating seismicity. Note the 2 strands of seismicity shown in the across fault section defining the NE and SW parallel strands. Both are populated with repeating earthquakes (indicating ongoing fault slip). The drilling plan proposes to drill subhorizontally from the SW to the NE into the M2 targets. Note that both M2 targets occur on the NE strand.

